



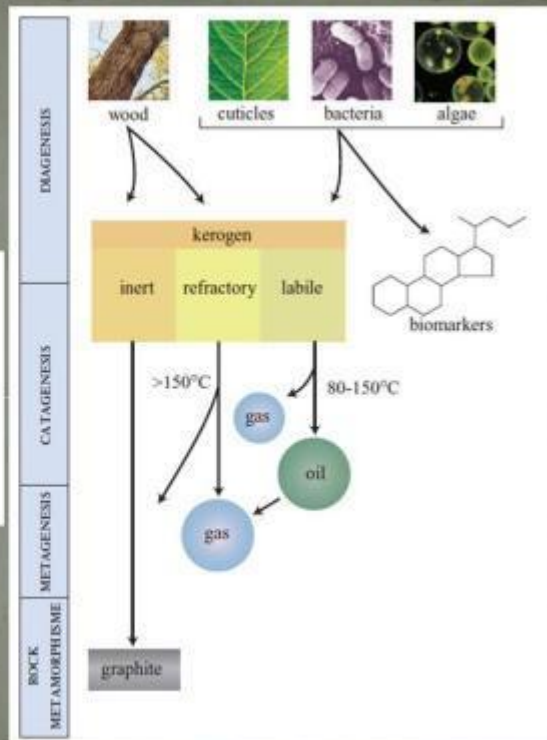
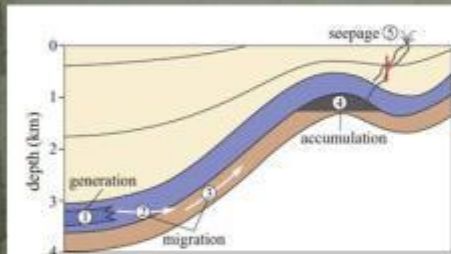
ΤΕΧΝΙΚΟ ΕΠΙΜΕΛΗΤΗΡΙΟ ΕΛΛΑΔΟΣ
ΤΕΕ/ΤΜΗΜΑ ΑΝΑΤΟΛΙΚΗΣ ΚΡΗΤΗΣ
ΤΕΕ/ΤΜΗΜΑ ΔΥΤΙΚΗΣ ΚΡΗΤΗΣ
ΠΕΡΙΦΕΡΕΙΑ ΚΡΗΤΗΣ
ΔΙΗΜΕΡΙΔΑ
«ΕΡΕΥΝΑ ΚΑΙ ΕΚΜΕΤΑΛΛΕΥΣΗ
ΥΔΡΟΓΟΝΑΝΘΡΑΚΩΝ ΣΤΗΝ ΕΛΛΑΔΑ»

ΤΕΕ

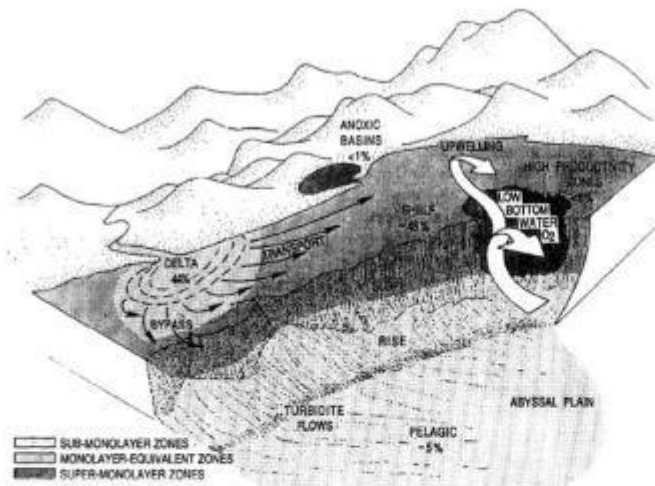


Μητρικά πετρώματα πετρελαίου και εκτεταμένες σπογγοαποικίες στην Κρήτη

Δρ. Μανούσογλου Εμμανουήλ
Γεωλόγος
Καθηγητής
Τμήμα Μηχανικών Ορυκτών Πόρων
Πολυτεχνείο Κρήτης



ENCYCLOPEDIA OF HYDROCARBONS, 2005



Major reservoirs of inorganic and organic carbon		
Reservoir type	Amount ^a	Reference
Sedimentary rocks		
Inorganic:		
Carbonates	60,000	Berner (1989)
Organic:		
Kerogen, coal, etc.	15,000	Berner (1989)
Active (areficial) pools		
Inorganic:		
Marine DIC	38	Olson et al. (1985)
Soil carbonate	1.1	Olson et al. (1985)
Atmospheric CO_2	0.66	Olson et al. (1985)
Organic:		
Soil humus ^b	1.5	Olson et al. (1985)
Land plant tissue ^b	0.95	Olson et al. (1985)
Seawater DOC	0.60	Williams and Druffel (1987)
Surface marine sediments	0.15	Emerson and Hedges (1988)

^a Unit = 10^{15} g C

^b Values corrected to levels before anthropogenic effects.

Idealized diagram depicting current estimates of the percentage of total organic matter burial occurring within various marine sediment types. *J.I. Hedges, R.G. Keil/Marine Chemistry 49 (1995) 81-115*

Oceanic productivity	$50 \times 10^{15} \text{ grC yr}^{-1}$
sediment burial rates	$0.16 \times 10^{15} \text{ grC yr}^{-1}$
Organic preservation in the marine environment	<0.5%
Shelf	~45%
Delta	44%
High productivity zones	<6%
Pelagic	~5%
Anoxic Basins	1%

J.I. Hedges, R.G. Keil/Marine Chemistry 49 (1995) 81-115

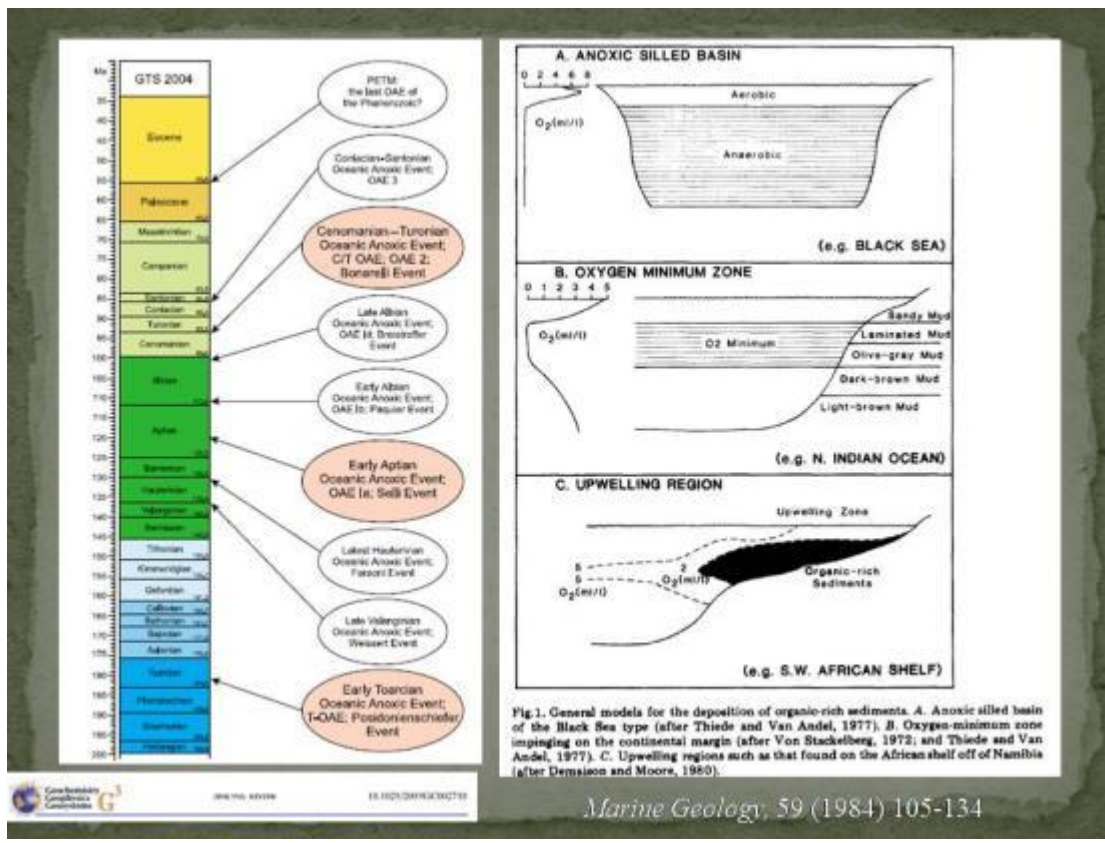
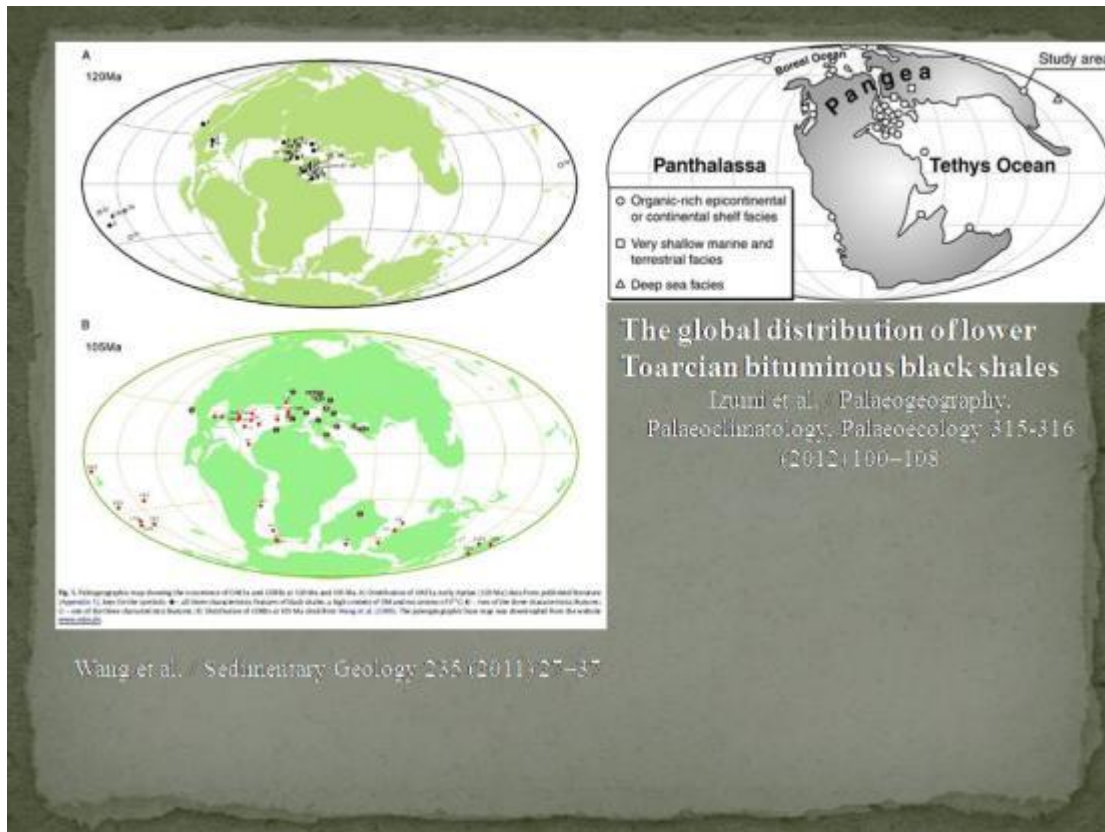


Fig. 1. General models for the deposition of organic-rich sediments. A. Anoxic silled basin of the Black Sea type (after Thiede and Van Andel, 1977). B. Oxygen-minimum zone impinging on the continental margin (after Von Stackelberg, 1972; and Thiede and Van Andel, 1977). C. Upwelling regions such as that found on the African shelf off of Namibia (after Demaison and Moore, 1960).

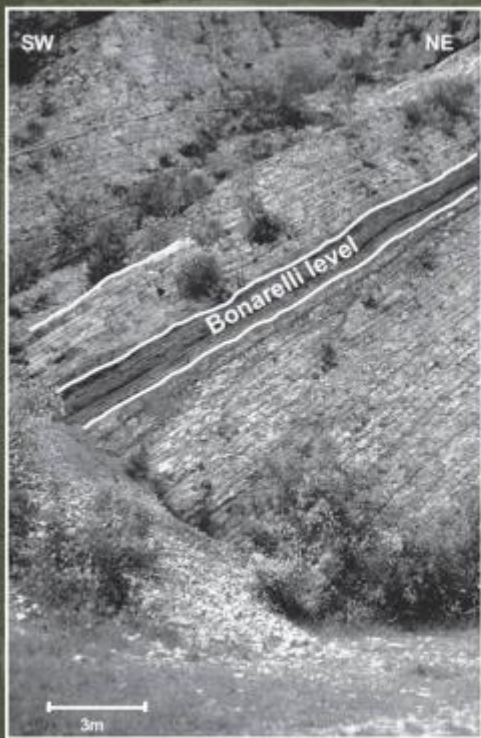
Cambridge University Press
 978 0 521 88002 3
 10.1017/C9780521880023

Marine Geology, 59 (1984) 105-134

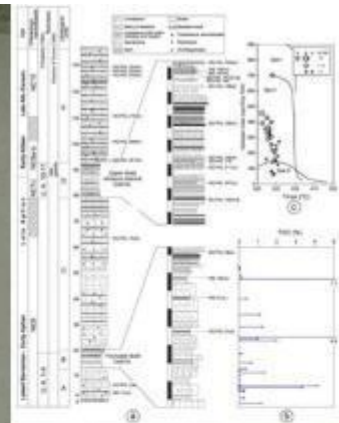




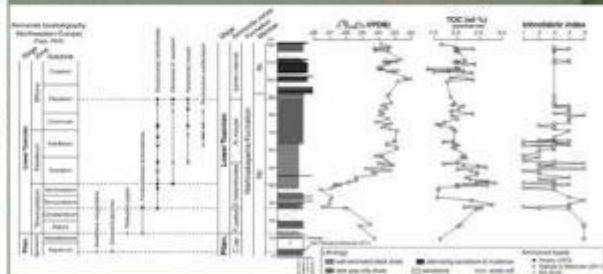
Wang et al. / Sedimentary Geology 235 (2011) 27–37



Cretaceous Research, 28, (2007) 597-612



Revue de Micropaléontologie 50 (2007) 225–237

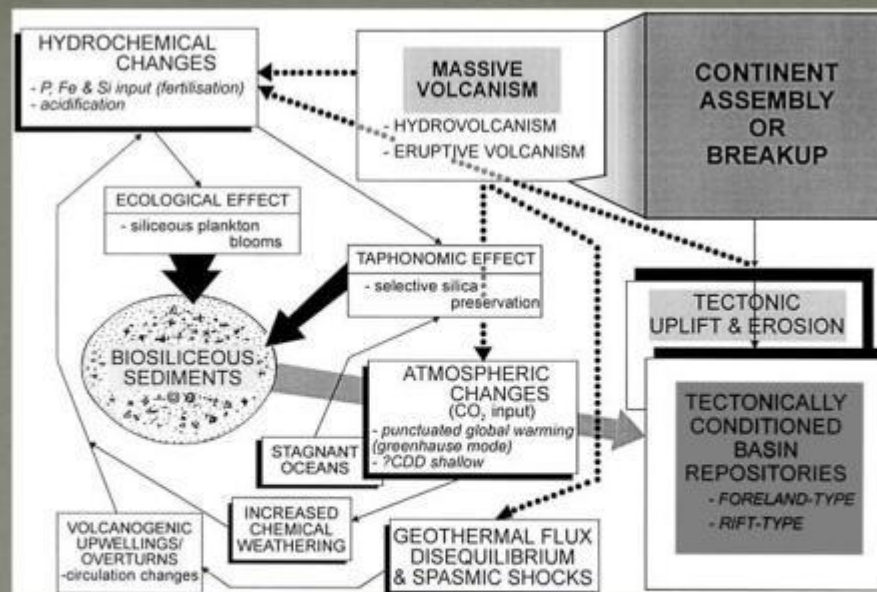


Izumi et al. / Palaeogeography, Palaeoclimatology, Palaeoecology 315-316 (2012) 100–108

Στον χώρο των Εξωτερικών Ελληνίδων εμφανίζεται από το Μέσο Τριαδικό αλλά κυρίως μετά το Ιουρασικό, μια συζυγία πετρωμάτων πυριτικής σύστασης στις Ζώνες Πίνδου, Ιόνιος, Παξών καθώς και στα μεταμορφωμένα πετρώματα των Πλακωδών Ασβεστολίθων (Πελοπόννησος, Κρήτη, Κάσος, Κάρπαθος, Ρόδος).

Ορισμοί - Ερμηνείες

- Πυριτόλιθοι - κερατόλιθοι
Ανόργανης (διαγενετικής) προέλευσης
ή
- “Ραδιολαρίτες”



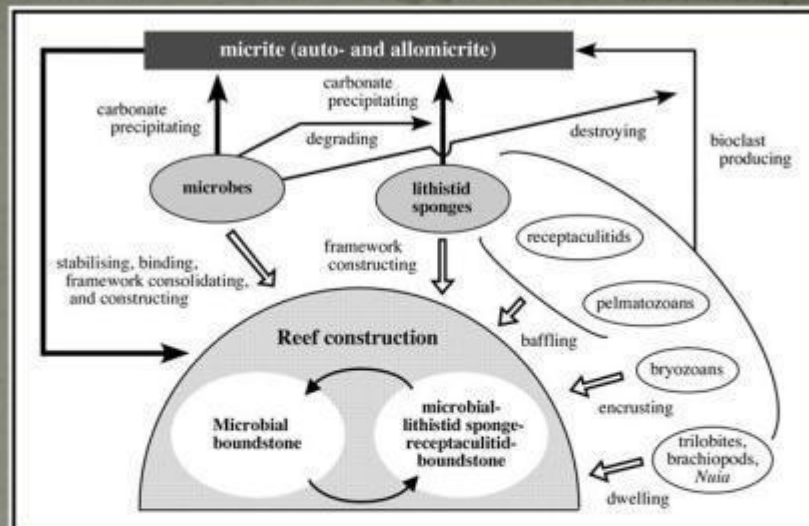
Flow chart for the model of massive volcanism and tectonics as a main control of biosiliceous sedimentation

G. Racki, F. Cordey, Earth-Science Reviews 52 (2000) 83–120

Ύφαλοι πυριτιοσπόγγων έχουν εμφανιστεί διαδοχικά στην εξελικτική πορεία του πλανήτη. Στο Ανώτερο όμως Ιουρασικό σχημάτισαν μια υφαλόγωνα αλυσίδα που επεκτάθηκε πάνω από 7.000 χιλ. Ο σημερινός ύφαλος που υπάρχει (Great Barrier Reef) στην Αυστραλία είναι σχετικά μικρός σε σχέση με αυτόν του Ανωτέρου Ιουρασικού. Το σύστημα αυτό των υφάλων αποτέλεσε την μεγαλύτερη βιοτική δομή που δημιουργήθηκε ποτέ πάνω στην Γη.



Paleogeographic situation during Late Jurassic. (Map used and modified after Blakey 2002)



Schematic model showing those elements that combined to construct the Lower Ordovician reefs, made up of microbial boundstones and microbial-lithistid sponge-receptaculitid boundstones. Micrites are a significant component of the reefs and are produced variously by microbes as well as skeletal organisms (lithistid sponges in particular).

N. Adachi et al. / *Sedimentary Geology* 220 (2009) 1–11

“The Late Jurassic records is one of the largest reefal expansions of the Phanerozoic, with a greater diffusion and differentiation in the Tethys realm”

Comparison of main morphological features and distribution of main biota along the depositional profiles of available examples from Intra-Tethys reef types

...zonation model for Upper Jurassic Intra-Tethys reef complexes. Rusciadelli et al. *Sedimentary Geology* 233 (2011) 69–87

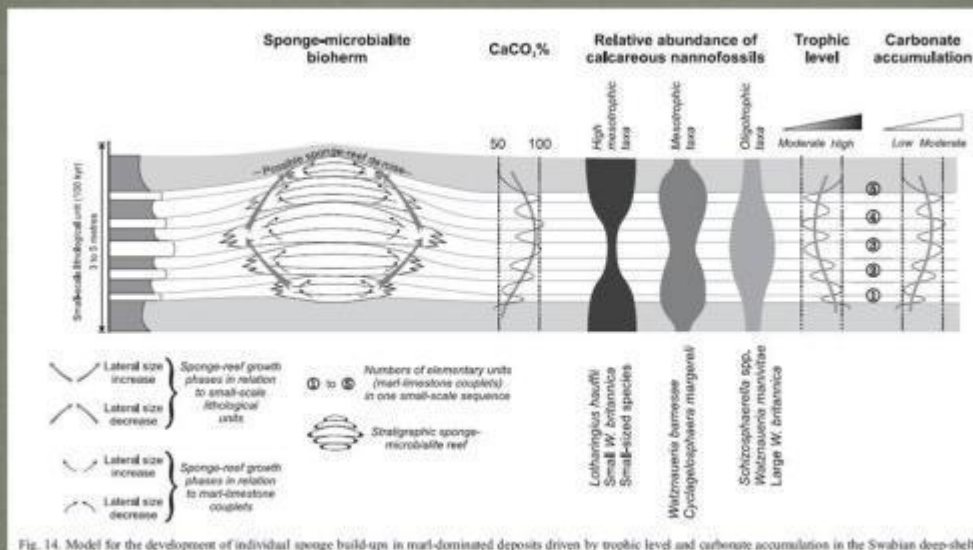
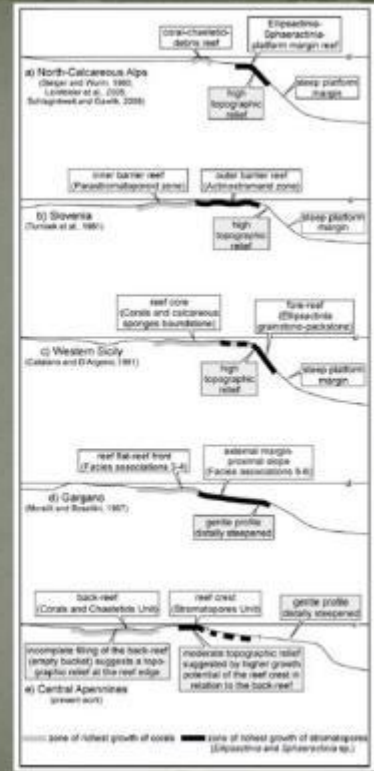
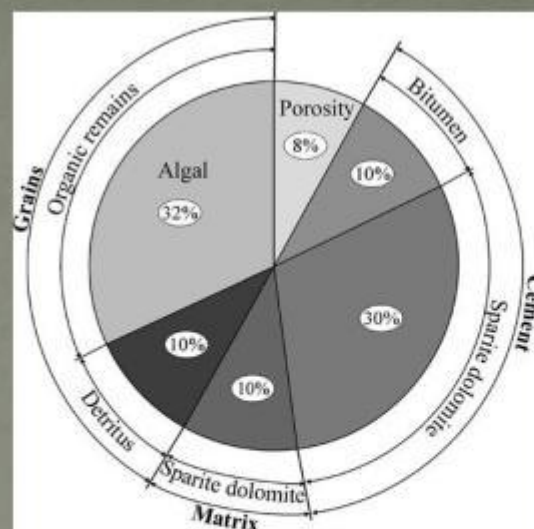


Fig. 14. Model for the development of individual sponge build-ups in marl-dominated deposits driven by trophic level and carbonate accumulation in the Swabian deep-shelf.

Olivier et al. / *Palaeogeography, Palaeoclimatology, Palaeoecology* 212 (2004) 233–263

- “The sediment within the sponge bioherms is characterized by a high levels of organic carbon. The large amount of organic carbon (**more than 3 weight percent**) found in the reef sediments is similar to that found at modern deltas on the west coast of Canada (Bornhold, 1978). Reducing conditions, which are usually observed in the recovered cores and grab samples in the shallow subsurface in reef sediments, are probably explained by this high organic carbon content. These dys- or anoxic conditions are responsible for the paucity and low diversity of endobenthic organisms” (Recent Hexactinellid Sponge Reefs on the Continental Shelf of British Columbia, Canada, <http://www.ponifera.org/vol11.htm>)

The link between black cherts and high biological activity is nearly systematic from the Precambrian to the Recent (van Kranendonk, 2001)

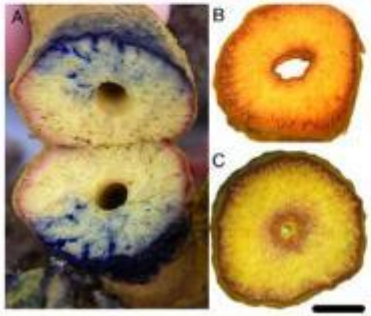
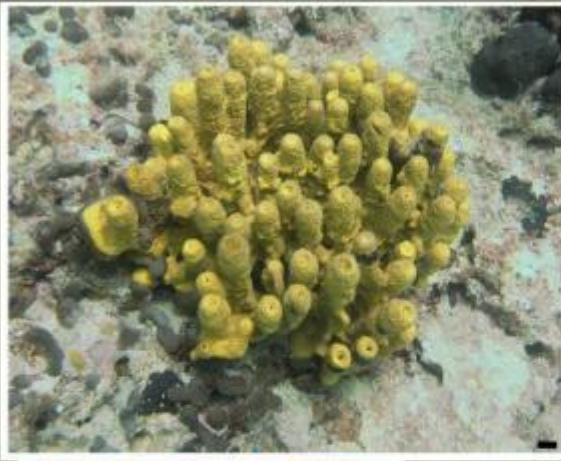


Organogenic build-up

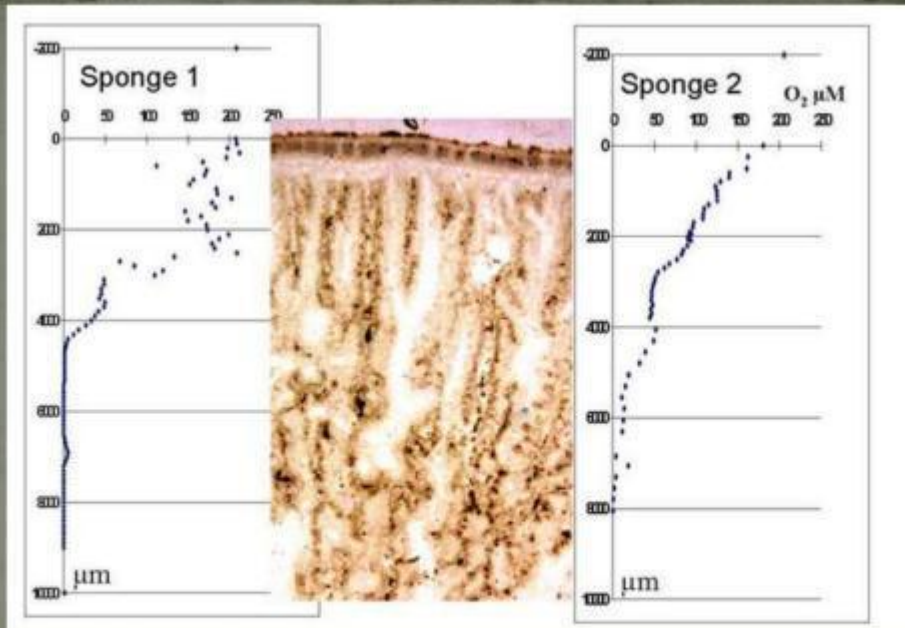
(Organic remain: algae, stromatoporoids, erinoids, gastropods, protozoans)

A lithofacies model for the Upper Devonian Pamyatno-Sasovskoye **reef (oilfield)** (Volgogradskoe Povolzhye, Russia)

S.V. Deliya, N.V. Danshina: *Palaeoworld* 19 (2010) 278–283

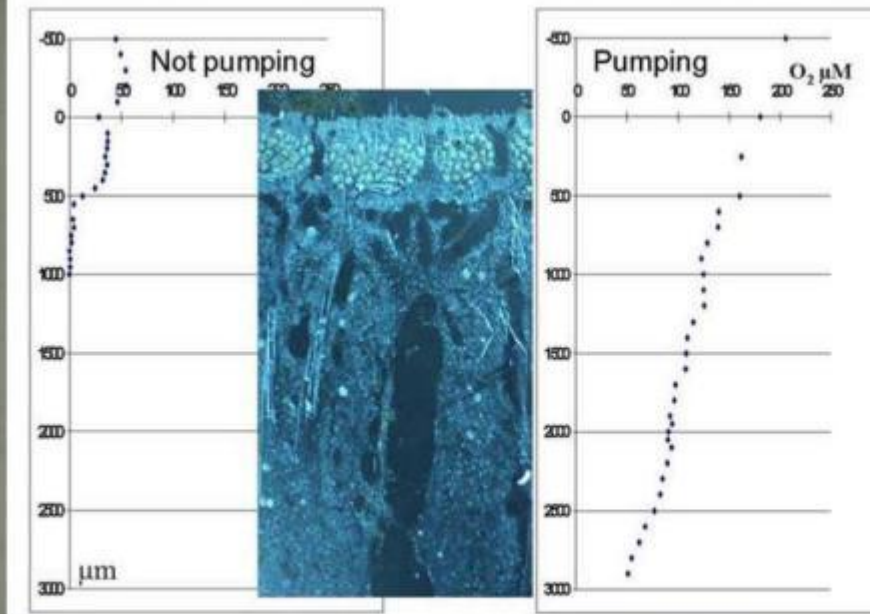


Journal of Experimental Marine Biology and Ecology, 369 (2009) 65–71



Oxygen profiles 1 cm into the tissue of two pumping *G. barretti* related to a microscopical sponge section of the same scale.

Microbial sulfate reduction in the tissue of the cold-water sponge Geodia barretti (Tetractinellida, Demospongiae), Dissertation, 2003

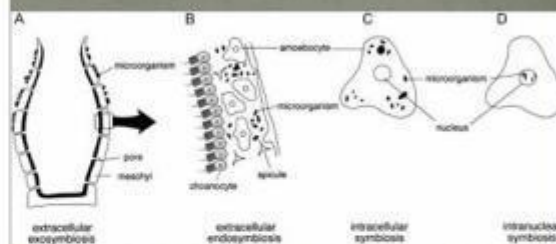


Oxygen profiles 3 mm into the tissue of sponge 2. related to a microscopical sponge section of the same scale.

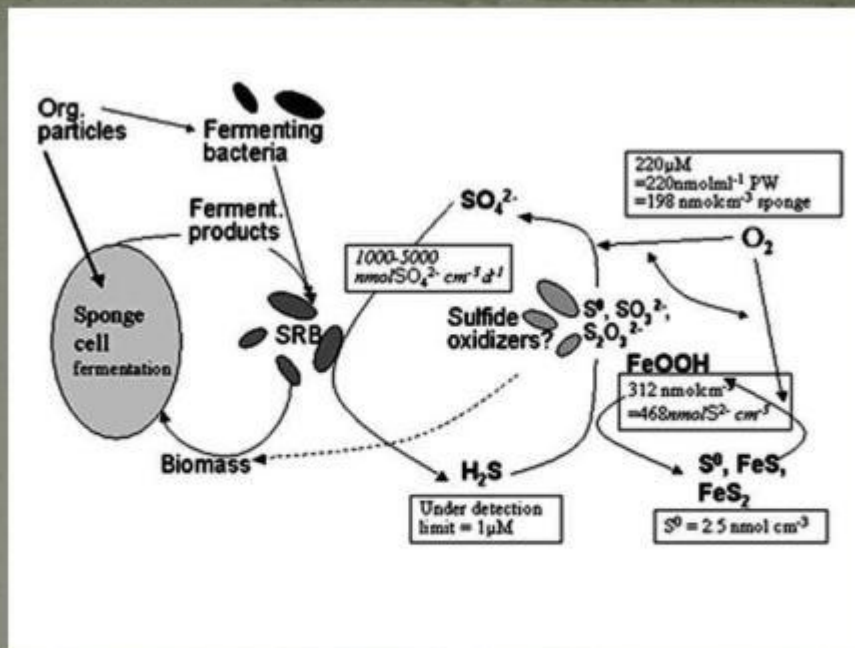
Microbial sulfate reduction in the tissue of the cold-water sponge *Geodia barretti* (Tetractinellida, Demospongiae), Hoffmann F., Dissertation, Göttingen, 2003

Table 2. Sponges and their symbiotic microorganisms producing natural products

Sponge	Symbiotic microorganism
<i>Actinia orientalis</i>	Filamentous bacteria
Antarctic sponge	B. <i>Pseudomonas aeruginosa</i>
<i>Aplysina</i> sp.	B. <i>Arctobacter</i> sp.
<i>Aplysina</i> sp.	B. <i>Bacillus</i> sp.
<i>Aplysina</i> sp.	B. <i>Micrococcus</i> sp.
<i>Aplysina</i> sp.	B. <i>Pseudomonas</i> sp.
<i>Aplysina</i> sp.	B. <i>Halo</i> sp.
<i>Coverclanum zymbicium</i>	Archeon
<i>Dysidea herbacea</i>	Cyanobacterium
<i>Dysidea herbacea</i>	C. <i>Oscillatoria spongeliae</i>
<i>Dysidea</i> sp.	B. <i>Halo</i> sp.
<i>Haliclonda olivata</i>	B. <i>Alteromonas</i> sp.
<i>Haliclonda olivata</i>	D. <i>Proocentrum</i> (bba)
<i>Haliclonda parvica</i>	B. <i>Antarcticum</i> (symbiont)
<i>Haliclonda parvica</i>	B. <i>Pseudomonas</i> sp.
<i>Haliclonda parvica</i>	B. <i>Rhodobacter</i> sp.
<i>Haliclonda parvica</i>	B. <i>Psychrospora burtonensis</i>
<i>Homophymia</i> sp.	B. <i>Pseudomonas</i> sp.
<i>Hymella</i> sp.	B. <i>Halo</i> sp.
<i>Rhopileutes odorabile</i>	B. β -Proteobacteria
<i>Rhopileutes odorabile</i>	B. γ -Proteobacteria
<i>Rhopileutes odorabile</i>	A. <i>Actinobacteria</i> sp.
<i>Rhopileutes odorabile</i>	B. <i>Cytophaga</i> sp.
<i>Rhopileutes odorabile</i>	Green sulfur bacteria
<i>Syngaster symbiotica</i>	R. <i>Ceratolycion spongelium</i>
<i>Siberia creba</i>	B. <i>Pseudomonas</i> sp.
<i>Siberia creba</i>	B. <i>Pseudomonas</i> sp.
<i>Tadusa sp.</i>	B. <i>Micrococcus</i> sp.
<i>Thaonella zimbouei</i>	B. δ -Proteobacteria
<i>Thaonella zimbouei</i>	C. <i>Aphanocapsa feldmannii</i>
<i>Thaonella zimbouei</i>	Filamentous bacteria
<i>Thaonella zimbouei</i>	Uncultured bacteria
Uncultured sponge	A. <i>Streptomyces</i> sp.
<i>Vinanga</i> sp.	B. <i>Alteromonas</i> sp.
<i>Vinanga</i> sp.	B. <i>Pseudomonas</i> sp.
<i>Zostera</i> sp.	B. <i>Alteromonas</i> sp.



Schematic diagram of symbiotic relationships between sponges and microorganisms. A. extracellular exosymbiosis; B. extracellular endosymbiosis; C. intracellular symbiosis; and D. intranuclear symbiosis. Microbial Symbiosis in Marine Sponges. Lee *et al.* J. Microbiol., Vol. 39, No. 4, 254-264.



Biological-chemical and sponge-bacteria interactions in the tissue of *G. barretti*.
Microbial sulfate reduction in the tissue of the cold-water sponge Geodia barretti
 (Tetractinellida, Demospongiae), Hoffmann F., *Dissertation*, Göttingen, 2003



How the sponge stays slim, *Nature* | doi:10.1038/news.2009.1088
 One species' rapid cell shedding explains its huge carbon-catching capacity.

De Goeij, J. M. *et al.*. Cell kinetics of the marine sponge *Halisarca caerulea* reveal rapid cell turnover and shedding. *J. Exp. Biol.* **212**, 3892-3900 (2009)

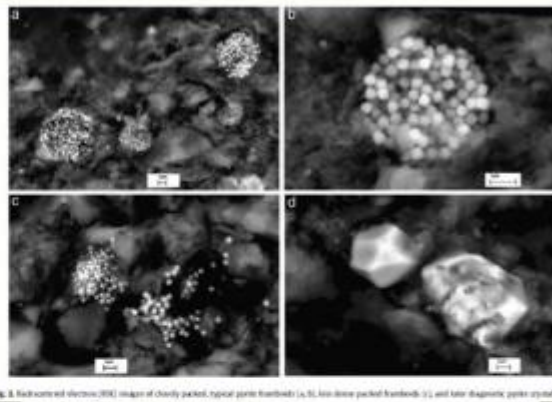
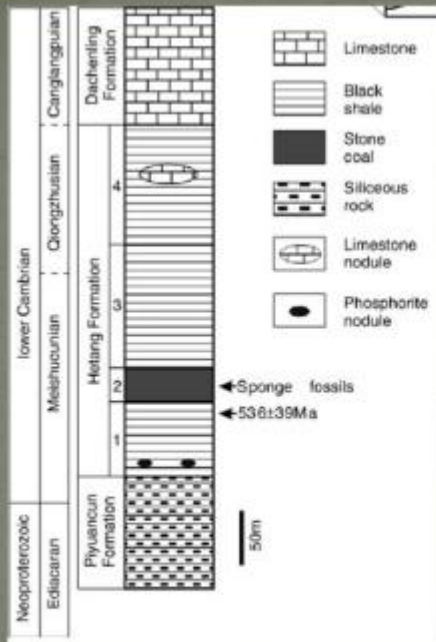


Fig. 8. Backscattered electron (BSE) images of (a) typical porous framework, (b) less dense packed framework, (c) and later diagenetic spicule crystals (d).

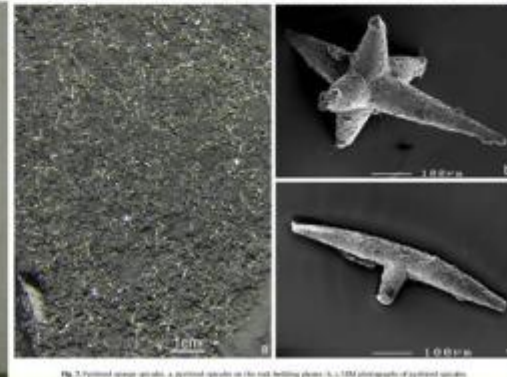
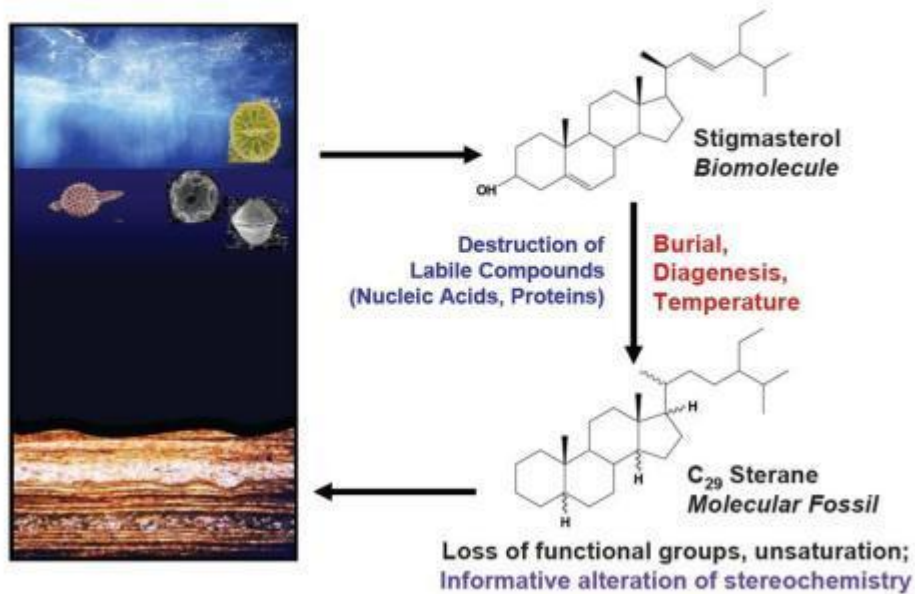


Fig. 9. Fossilized sponge spicules, a porous sponge on the left, Hetiang phase, 53.6 Ma; SEM photographs of spined spicules.

Palaeogeography, Palaeoclimatology,
Palaeoecology
271 (2009) 279–286

The Biomarker Principle



Roger E. Summons, MIT

- Petroleums and bitumens from Early Proterozoic (1800 Ma) to Miocene (15 Ma) age marine strata contain 24-isopropylcholestanes**, a novel group of C₃₀ steroids. The abundance of these compounds, relative to 24-n-propylcholestanes, varies with source rock age. Late Proterozoic (Vendian) and Early Cambrian oils and/or bitumens from Siberia, the Urals, Oman, Australia, and India have a high ratio of 24-isopropylcholestanes to 24-n-propylcholestanes (>1), while younger and older samples have a lower ratio (<0.4). **Temporal changes in this parameter may reflect the relative abundance of certain Porifera (sponges) and certain marine algae through time.** Geochemical indicators such as this, which can constrain the source rock age of a migrated oil, are useful in source rock identification during petroleum exploration.

Paleoenvironmental implications of novel CM steranes in Precambrian to Cenozoic age petroleum and bitumen,
 McCaffrey et al., *Geochimica et Cosmochimica Acta*, 1994, Vol. 58, pp. 529-532

Table 1 Distributions of selected biological markers in reef carbonates and associated organisms

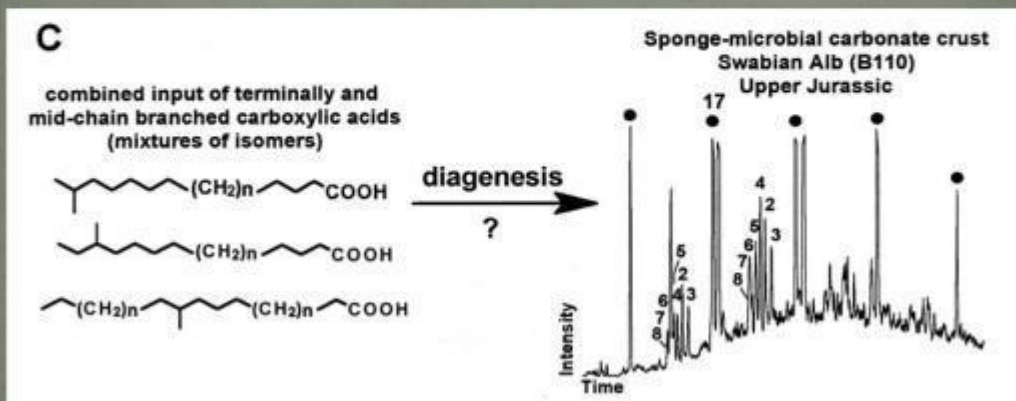
COMPOUND	STRUCTURE	FEATURE	ORIGIN	SAMPLES								
				'Cyanobacterial facies'				Reef carbonates (marine)		Sponges		
				Cultures	Carbonates (recent)	Carbonates (fossil)	Microbialites	Others	Agarites	Others		
n-Heptacosane		high relative abundance	Cyanobacteria	XX	XX	XX	XX	X	X	XX		
n-Heptacosane		high relative abundance	Cyanobacteria	XX	XX	XX	XX			XX		
n-Octacosane		high relative abundance	Green algae (?)							XX	XX	
Mit-chain br. alkanes		diatomic isomers	Cyanobacteria	XX	XX	XX	XX	XX	XX	X		
Diethyl-alkanes		presence	Cyanobacteria							XX		
Diisoprenes		high relative abundance	Cyanobacteria	X	X	XX	X	XX	XX	X		
Short-chain n-alkanes		modal distributions	Microbialites?					XX	XX	XX	X	X
Mit-chain br. alkanes		complex mixtures	Microbialites?					XX	XX	XX	X	X
Linear fatty acids <C25		high relative abundance	widespread	XX	XX	XX	XX	XX	XX	XX	X	XX
Terminally br. fatty acids		presence	Amoebae, bacteria	X	X	X	X	X	X	X	X	XX
Mit-chain br. fatty acids		presence	Microbialites					XX	XX	XX	X	XX
Demersoprenic acids		presence	Demersoprenes					XX	XX	XX		
Highly br. isoprenoids		presence	Diatoms					XX	XX	XX		
Cholesterol		presence	Animals, algae	XX	X	X	X			XX	XX	XX
n-1-sterols		presence	Animals, sponges							XX	XX	XX
Halogenated compounds		presence	Sponges							XX	XX	XX
n-alkanes <C25 (nd)		high relative abundance	Higher plants	X	XX	XX	XX	X	X	XX	X	XX

Explanations

XX = main compound / pronounced feature
 X = minor relative abundance / subordinate feature
 Y = trace compound
 o = compound fraction not analyzed
 no entry: compound / feature absent or below detection limit
 br. = branched

Thiel et al., (1996): Biogeochemistry of Modern Porifera and Microbialites from Lizard Island (Great Barrier Reef, Australia) and Fossil Analogues. In: Reitner et al., *Globale und regionale Steuerungsfaktoren biogener Sedimentation*. Gött.Arbeitskreis Geol. Paläont. SB2, 129-132; Göttingen.

“The found mid-chain branched carboxylic acids represent potential biological precursors for series of mid-chain branched alkanes present in ancient sediments and oils”



Mid-chain branched alkanolic acids from “living fossil” demosponges: a link to ancient sedimentary lipids? Thiel et al. *Organic Geochemistry* 30 (1999) 1-14.

nature

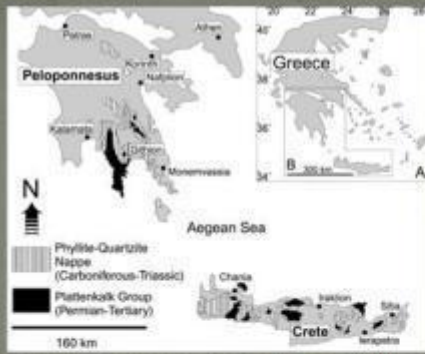
Vol 457 | 5 February 2009 | doi:10.1038/nature07673

LETTERS

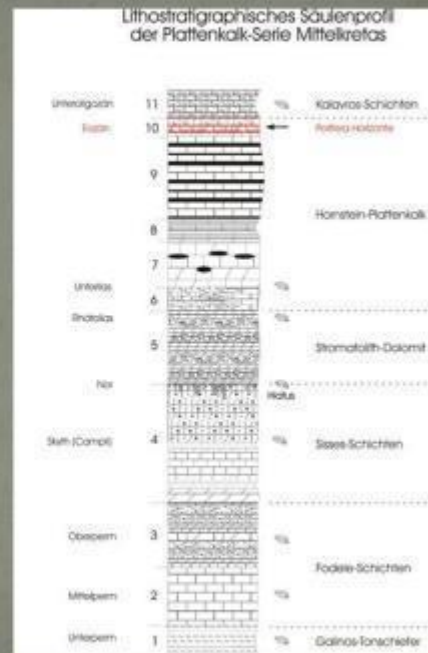
Fossil steroids record the appearance of Demospongiae during the Cryogenian period

Gordon D. Love^{1,2}, Emmanuelle Grosjean³, Charlotte Stalvies⁴, David A. Fike⁵, John P. Grotzinger⁵, Alexander S. Bradley¹, Amy E. Kelly², Maya Bhatia³, William Meredith⁶, Colin E. Snape⁶, Samuel A. Bowring³, Daniel J. Condon^{3†} & Roger E. Summons³

“...C30 steranes comprised 2.7% of total C27–C30 extractable steranes in Huqf samples and 63% of the summed C30 compounds were 24-isopropylcholestanes, suggesting *that demosponges must have made a significant contribution to preserved sedimentary organic matter...*”

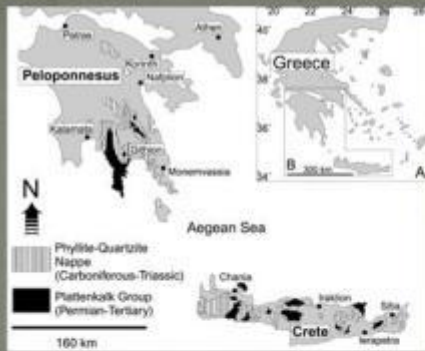


MANUŞOĞLU E., SOUJON A., REITNER J. & DORNSIEPEN U.E. (1995) Relikte Lithistiden Demospongien aus der metamorphen Plattenkalk-Serie der Insel Kreta (Griechenland) und ihre paläobathymetrische Bedeutung. - N. Jb. Geol. Palaeont. Mh., 1995/4: 235-247.

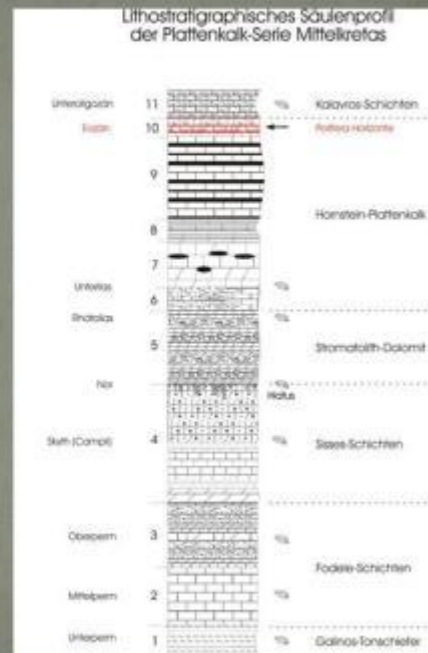


Εκτεταμένες σπηλαιοποιίες στην Ν.Ι.Α. ΨΗΛΟΡΕΙΤΗΣ



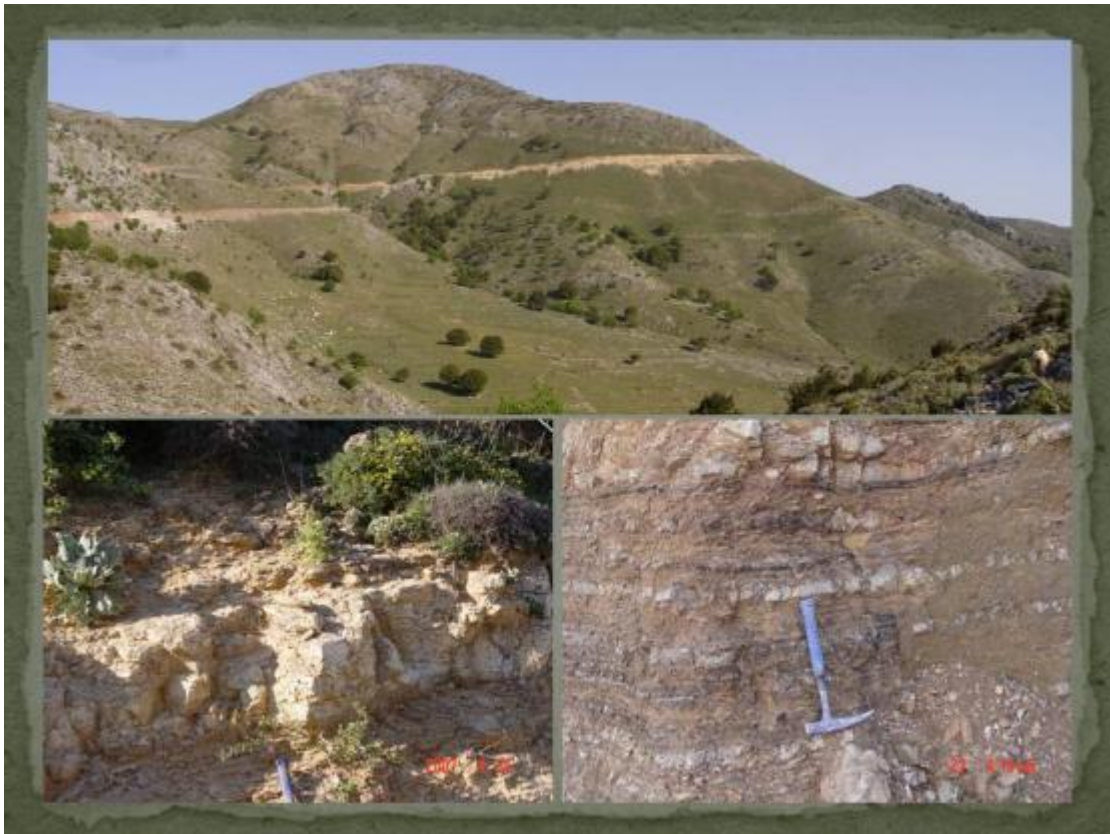


SOUFON A., MANUTSOGLU E., REITNER J. & JACOBSSHAGEN V. (1995): Lithostiride Demospongiae aus der metamorphen Plattenkalk-Serie der Trypali Ori (Kreta Griechenland). - Berliner geowiss. Abh., E, 16: 559-567, Berlin.



Εκτεταμένες απορροσποικίες στον δρόμο προς Ασφένδο, Α. Λευκά Όρη

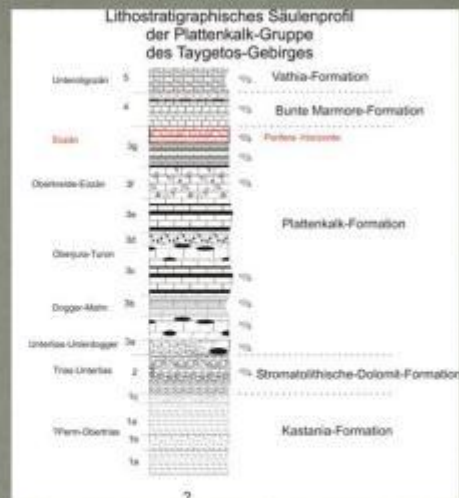


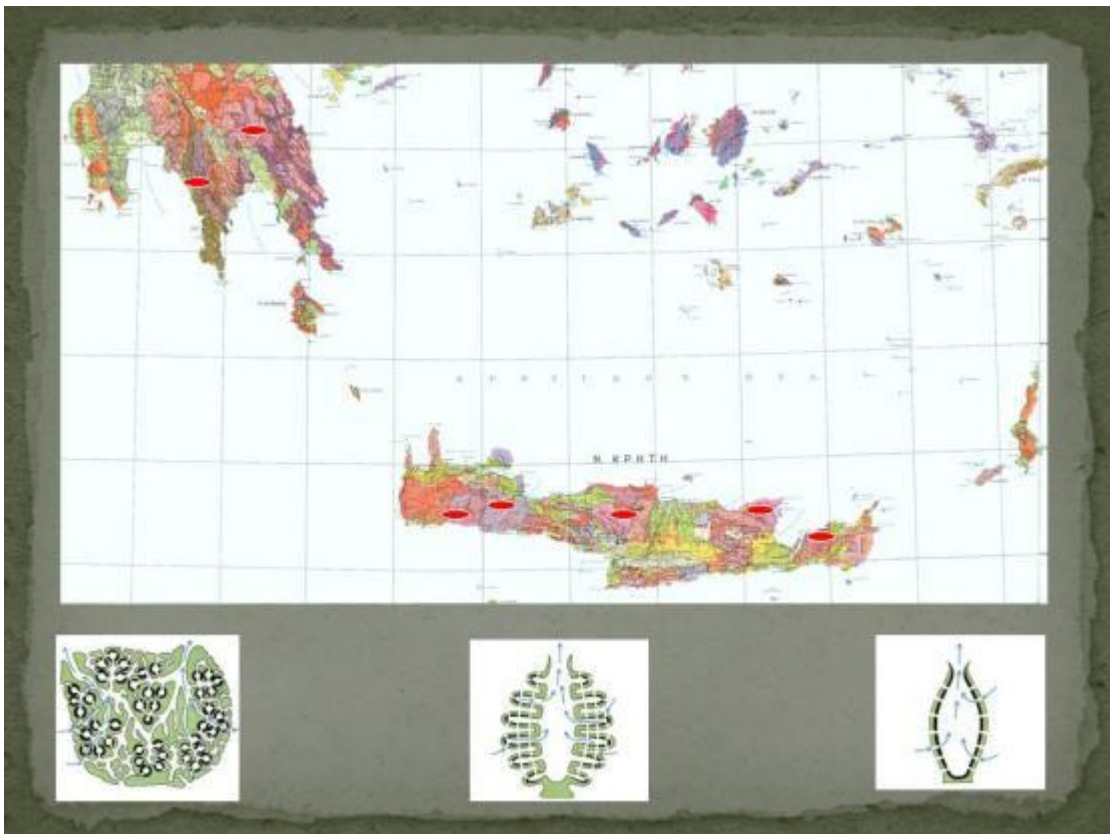


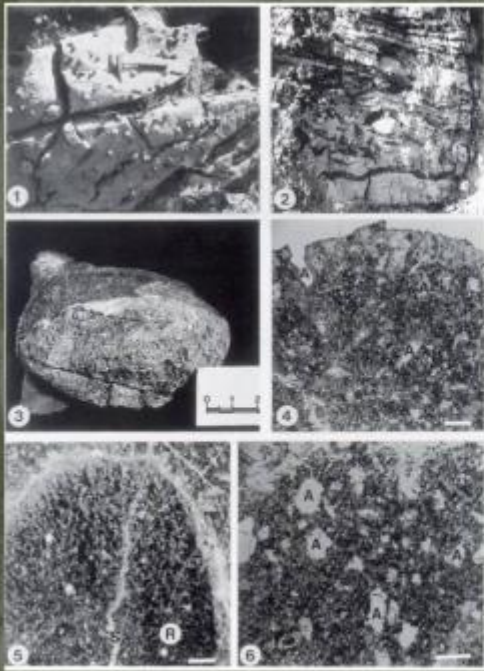
Διαφορετικές μορφές σπογγιοποικίων εντός του
Ευθικού Δρυϊνού Λευκών Ορέων



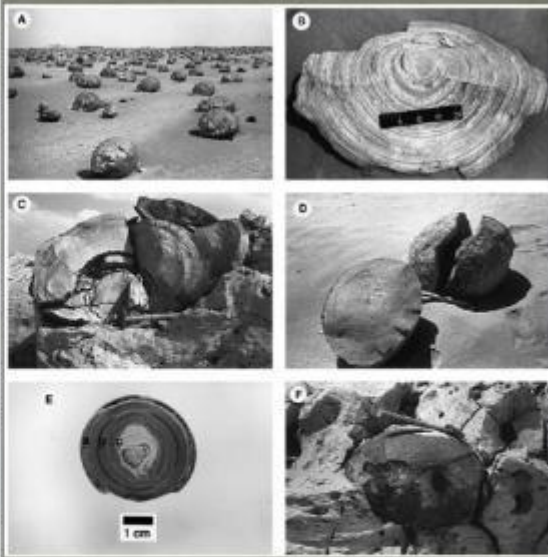
MANUSOGLU E., REITNER J.,
MARIOLAKOS D., BELLAS S.M.
& MARIOLAKOS I. (1998) Erster
Nachweis von Relikten lithistider
Demospongiae aus der Plattenkalk-
Gruppe des Taygetos-Gebirges,
Peloponnes Griechenland. - Z. dt.
geol. Ges., 149: 91-103, Stuttgart.



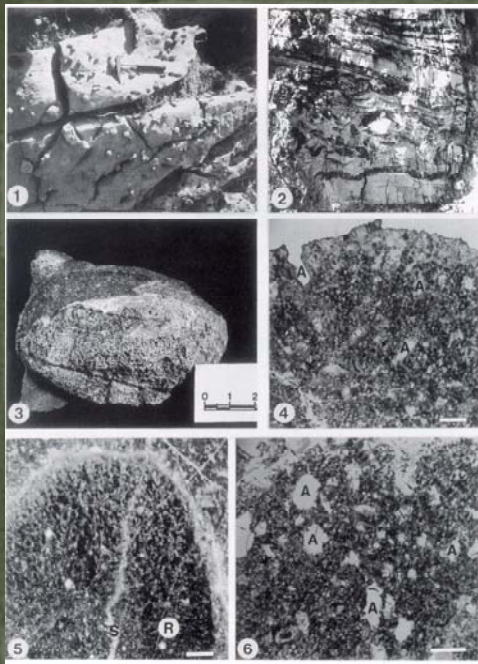




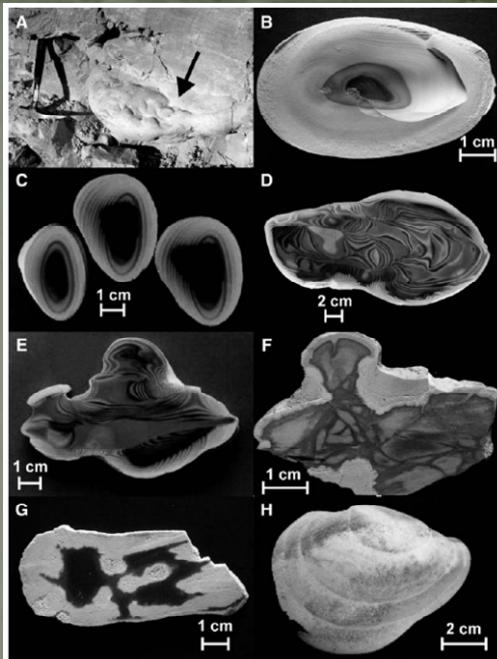
Soujon et al. (1995)
 Berliner geo. Abh., E, 16: 559-567



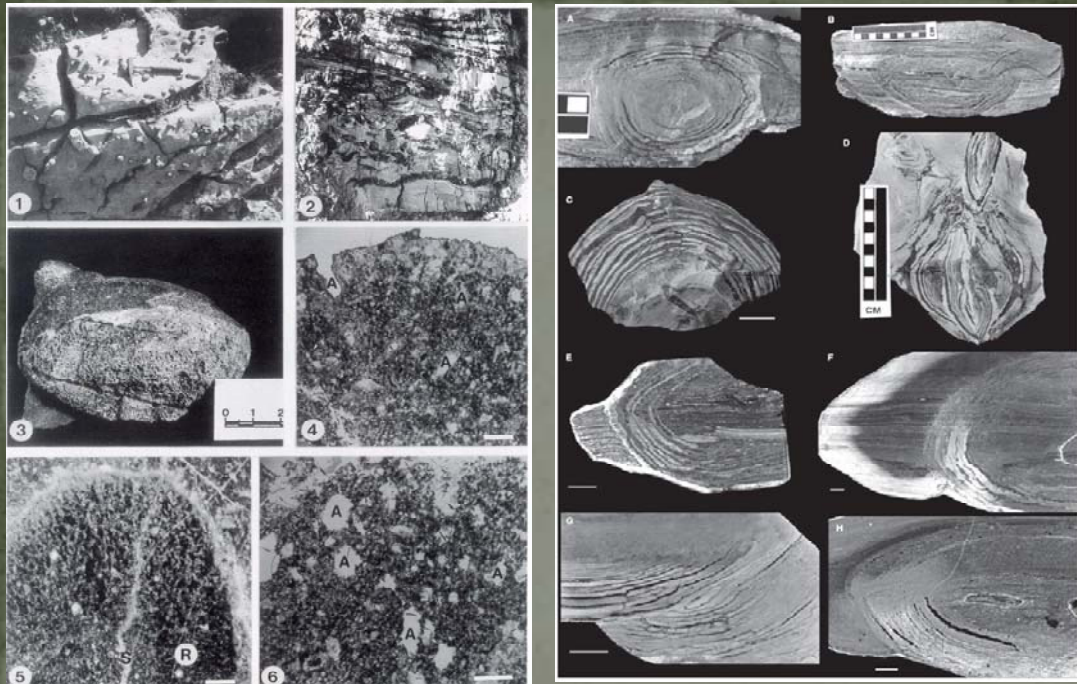
McBride et al. (1999)
 Sedimentology 46, 733-755
 Drunka Formation, Egypt
 (Lower Eocene)



Soujon et al. (1995)
 Berliner geo. Abh., E, 16: 559-567



Migaszewski et al. (2006)
 Sedimentary Geology, 187 11-28
 (Holy Cross Mountains, South-central Poland)



Soujon et al. (1995)
 Berliner geo. Abh., E, 16: 559-567

R. J. Behl (2010), Sedimentology,
 doi: 10.1111/j.1365-3091.2010.01165.x
 Monterey Formation of California
 Miocene

Source rock analysis by pyrolysis gas chromatography on siliceous and argillaceous rocks from Ajigasawa of Aomori area, Japan

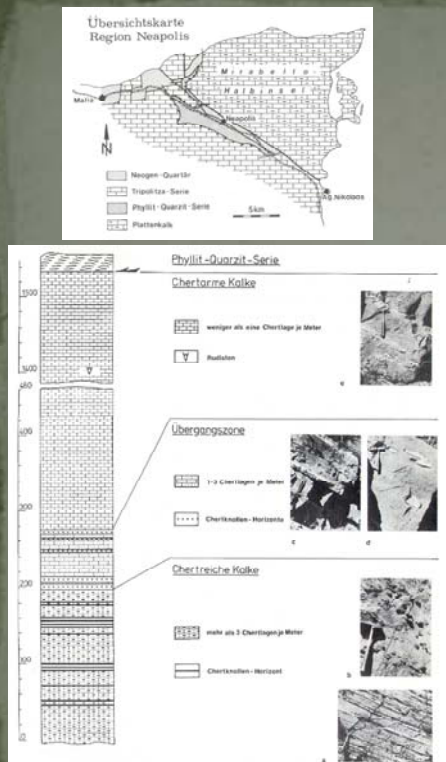
Sample No.	Lithology	Formation	T_{max} (°C)	TOC (%)	S_1 (%)	S_2 (%)	S_3 (%)	S_2/S_3	ρ_g (g/cm ³)	Φ (%)	k_a (md)
I-5A	Diatomite	Maido	400	0.55	0.78	1.27	0.47	2.7	2.32	64.6	3.9
I-3B	Diatomite	Maido ?	384	1.35	0.62	1.95	0.09	21.7	2.29	61.9	1.6
G-65.5	Diatomite	Maido	393	0.88	0.34	0.90	0.06	15.0	2.39	51.8	0.0
D-10	Diatomite	Akaishi	386	0.89	0.40	0.95	0.06	15.8	2.38	49.4	0.0
G-38C	Sil. shale	Akaishi	409	0.94	0.30	1.72	0.00	-	2.52	30.2	0.0
G-34	Sil. shale	Akaishi	417	1.17	0.55	3.86	0.19	20.3	2.47	26.7	0.0
G-20	Sil. shale	Akaishi	416	0.99	0.23	2.37	0.00	-	2.56	24.7	0.0
G-18B	Sil. shale	Akaishi	421	1.43	0.63	4.86	0.22	22.1	2.50	25.5	0.0
G-9D	Sil. shale	Ohdoji	420	2.76	0.79	16.31	0.73	22.3	2.48	26.4	0.0
G-2B	Sil. shale	Ohdoji	408	2.23	1.81	16.74	0.50	33.5	2.50	25.0	0.0
K-17.5	Sil. shale	Ohdoji	-	1.71	1.05	4.54	0.07	64.9	2.27	36.9	0.0
M-22	Sil. shale	Ohdoji?	406	0.42	0.21	0.51	0.18	2.8	2.51	28.3	75
G-15	Chert	Akaishi	416	0.86	0.56	1.86	0.04	46.5	2.49	19.2	0.7
K-25B	Chert	Ohdoji	-	1.72	1.52	7.30	1.94	3.8	2.19	21.9	0.1
K-19B	Chert	Ohdoji	-	1.88	0.97	5.87	1.40	4.2	2.21	27.3	0.0
G-9L	Chert	Ohdoji	417	2.30	0.81	13.05	0.81	16.1	2.52	29.1	0.5
G-41B	Siltstone	Akaishi	407	0.60	0.27	0.76	0.33	2.3	2.31	29.0	0.0
M-37B	Claystone	Akaishi ?	390	0.97	0.50	1.14	0.14	8.1	2.24	39.4	0.6
K-10	Mudstone	Ohdoji	-	0.44	0.33	0.60	0.88	0.7	2.40	29.1	0.0
K-8	Siltstone	Ohdoji	437	0.48	0.44	0.90	0.24	3.7	2.55	40.6	-
M-3	Mudstone	Tanosawa ?	404	0.75	0.27	0.46	0.21	2.2	2.53	27.2	-

Journal of Petroleum Science and Engineering, 7 (1992) 247-262

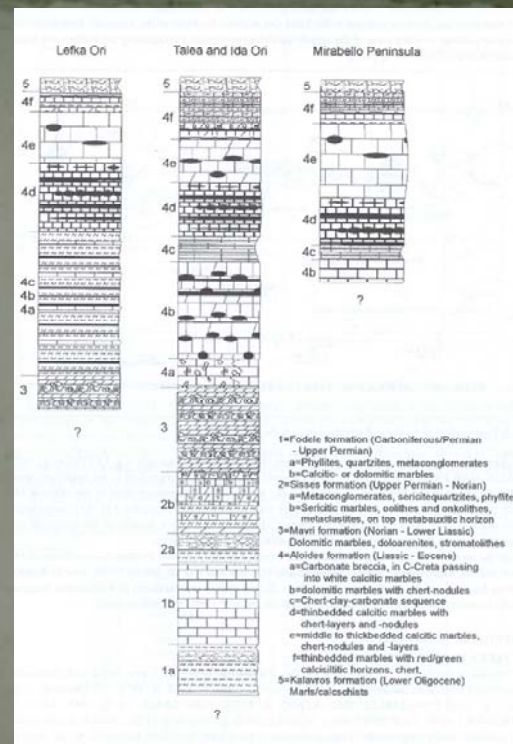
Sample no.	Cherts (the Shangsi Section, Guangyuan Area)				
	159-1	156-1	155-2	154-3	154-1
TOC	2.72	2.43	2.19	1.35	7.49
Ti	256.79	294.96	289.76	227.45	840.53
Al	7188.72	8706.06	8586.23	7279.89	21,895.24
T Fe	3604.13	8741.59	6000.05	6231.89	18,632.49
Mn	72.96	46.21	68.04	143.21	55.9
P	523.03	149.94	489.23	313.13	830.82
Mg	2460.92	3043.66	8552.09	5392.54	2462.22
Ca	159,854.56	69,111.87	103,152.81	245,783.47	9318.47
K	1322.6	1231.32	1565.28	1958.11	4354.16
Cd	12.36	11.42	11.65	0.38	19.18
V	323.64	741.55	331.38	95.73	466.1
Cr	79.25	154.13	88.49	12.04	120.99
Co	3	7.09	4.43	1.44	4.25
Ni	36.92	90.47	47.61	11.1	83.6
Cu	48.52	31.26	43.27	5.22	39.4
Zn	36.23	54.31	36.88	10.71	60.24
Rb	9.54	11.17	11.32	2.91	10.07
Sr	1284.77	739.4	2045.77	541	896.15
Y	4.7	7.23	8.3	2.09	14.69
Zr	13.87	23.34	27.65	8.04	18.12
Mo	22.77	213.61	32.32	23.69	73.16
Pb	2.09	3.73	3.33	1.23	2.75
Th	0.83	1.23	1.31	0.54	1.1
Ba	39.72	45.4	42.34	7.71	92.41
Ga	1.66	1.98	1.89	0.57	1.74
U	10.39	21.02	15.77	3.27	23.74

Elements in ppm; TOC in %.

Chen et al. (2012) Journal of Geochemical Exploration, 112, 35-53



Wachendorf et al, 1980



(Soujon, Jacobshagen & Manutsoglu, 1998)

Σας ευχαριστώ πολύ για
την προσοχή σας